Biosensors and Bioelectronics 26 (2011) 2520–2526

Contents lists available at ScienceDirect

Biosensors and Bioelectronics

journal homepage: www.elsevier.com/locate/bios

An electrical biosensor for the detection of circulating tumor cells

Yao-Kuang Chung*,[1], Julien Reboud[2], Kok Chuan Lee, Hui Min Lim, Pei Yi Lim, Karen Yanping Wang, Kum Cheong Tang, HongMiao Ji, Yu Chen

*Institute of Microelectronics, A*STAR (Agency for Science, Technology and Research), 11 Science Park Road, Singapore Science Park II, Singapore 117685, Singapore*

ARTICLE INFO

Article history:
Received 16 July 2010
Received in revised form 6 October 2010
Accepted 27 October 2010
Available online 4 November 2010

Keywords:
Circulating tumor cells (CTC)
Immunomagnetic
Microelectrode array (MEA)

ABSTRACT

In this report, we demonstrate a semi-integrated electrical biosensor for the detection of rare circulating tumor cells (CTCs) in blood. The sample was first enriched through a combination of immunomagnetic isolation and size filtration. The integration of both methods provided a high enrichment performance with a recovery rate above 70%, even for very low numbers of cancer cells present in the original sample (10 spiked MCF7 cells in 0.5 mL of blood). In the same system, the sample was then transferred to a microchip for further magnetic concentration, followed by immunochemical trapping and electronic detection by impedance spectroscopy. Three levels of spiked CTC number (30 ± 2, 124 ± 29, 273 ± 23) in 10 μL of filtered blood sample were distinguished by monitoring the impedance change of the microelectrode array (MEA). The integration of different functions in a single system provided a methodology to process milliliter-sized blood samples at the macroscale and interface with the microdimensions of a highly sensitive electronic detector. The results showed that the whole system was able to detect different levels of spiked cancer cells without the use of time- and cost-intensive fluorescence labeling and image analysis. This has the potential to provide clinicians with a standalone system to monitor changes in CTC numbers throughout therapy conveniently and frequently for efficient cancer treatments.

1. Introduction

Metastasis, the spread of cancer from a primary tumor to another location or organ through the bloodstream or the lymphatic system, is a dramatic progression of the disease, resulting in treatment difficulties and high mortality. Previously, a metastatic spread was thought to be a late process in malignant progression, but recent work has shown that circulating tumor cells (CTCs) can shed in the blood at an early stage (Hüsemann et al., 2008). Their number in blood has been shown to be a mark of the aggressiveness of the disease, with clinical relevance in patient survival (Hayes et al., 2006). In 2008, the United States Food and Drug Administration (FDA) cleared the way for a system (CellSearch™, Veridex) which informs on the level of CTCs for metastatic breast cancer patients (Cristofanilli et al., 2004). The importance of CTCs has since been extended to the monitoring of cancer therapies (Pachmann et al., 2005a,b). These studies have confirmed the relevance of CTC levels as a diagnostic, prognostic or monitoring tool and highlight the importance of the availability of a sensitive, convenient and widely affordable system for their detection.

The major technical challenge for CTC detection is to enrich and then to identify rare CTCs in blood. Even for patients at an advanced stage, the CTC counts may only be hundreds to a few thousands per milliliter of blood, which contains millions of leukocytes and billions of erythrocytes (Allard et al., 2004; Fan et al., 2009). The selectivity and sensitivity needed for CTC detection require extensive sample preparation. Existing enrichment methods include density gradient (Baker et al., 2003), size filtration (Vona et al., 2000; Zheng et al., 2007), immunomagnetic separation/isolation (Benez et al., 1999; Talasaza et al., 2008; CellSearch™ system, Veridex), dielectrophoresis (DEP) (Gascoyne et al., 2009), and immunochemistry coupled with specific microfluidic designs (Nagrath et al., 2007; Wang et al., 2009).

Although CTCs can be differentiated from normal blood cells via density gradients, significant loss of cells can be encountered with their migration to the layer of blood plasma. Many CTCs also differ from other cells in the blood because of their larger size which allows them to be filtered out from blood cells by membranes with a pore size of 8 μm (Vona et al., 2000). Though size filtration is convenient and straightforward, its efficiency is still limited, as many white blood cells may remain on the membrane while smaller CTCs get filtered out. This is mostly due to the fact that the size of CTCs can range from 4 to 30 μm, even in a single patient (Allard et al., 2004).

* Corresponding author. Tel.: +886 2 2693 3232x17; fax: +886 2 8695 1411.
E-mail addresses: ykchung@ms.mainz.com.tw, yaokuangchung@gmail.com (Y.-K. Chung).
[1] Present address: 7F., No. 29-1, Ln. 169, Kangning St., Xizhi City, Taipei County 221, Taiwan. Maria Von Med-Biotechnology Co., LTD
[2] Present address: Division of Bioengineering, School of Engineering, Rankine Building, Oakfield Avenue, University of Glasgow, G12 8LT, United Kingdom.

0956-5663/$ – see front matter © 2010 Elsevier B.V. All rights reserved.
doi:10.1016/j.bios.2010.10.048

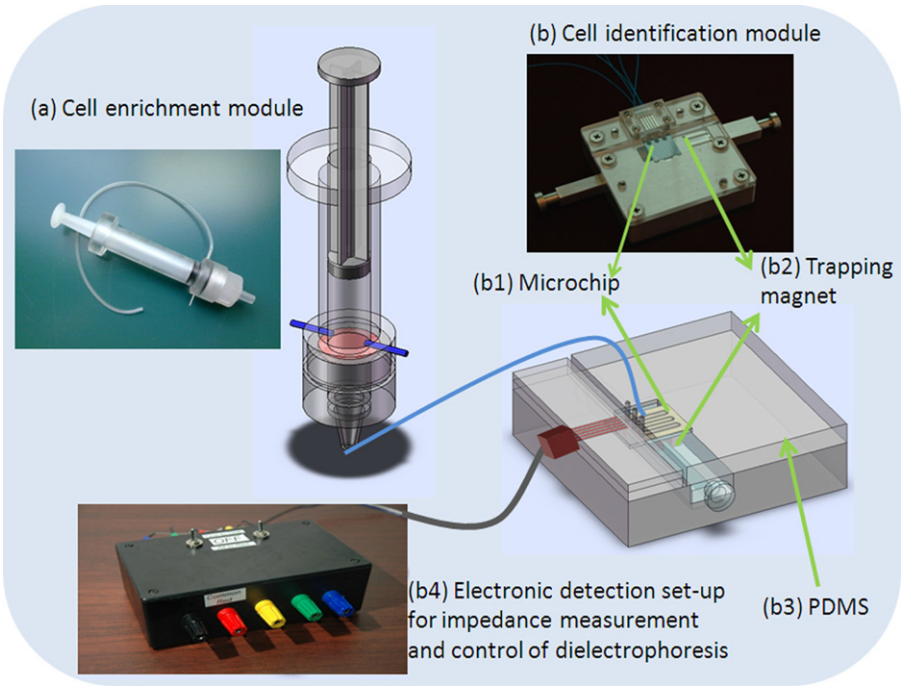

Fig. 1. Schematic design of the integrated system, including (a) Cell enrichment module, (b) Cell identification module consisting of (b1) the silicon microchip, (b2) a trapping magnet, (b3) a PDMS top cover to form the ceiling of the microchannels, and (b4) the electronic detection set-up for impedance measurement and control of dielectrophoresis.

Gascoyne et al. (2009) attempted to use potential differences in dielectric properties of cancer cells and blood cells to sort out CTCs, but the isolation efficiencies need to improve for practical sample processing of large volumes. Recent developments have been made to enhance the capture of CTCs on the surface of microchips by antibody-antigen interactions, using micropillars (Nagrath et al., 2007) and nanostructuration of the surface (Wang et al., 2009). However, the use of surface capture has hampered the throughput of these approaches. To increase the processing volume, the contact probability between the CTCs and the capture surface with specific antibody coating has to be enhanced. Immunomagnetic separation/isolation by using magnetic beads (Benez et al., 1999; Talasaza et al., 2008) has become a method of choice for the purification of clinical samples, but its integration with convenient detection systems is still lacking due to challenges in cell labeling and labor-intensive image analysis.

After the enrichment process, most systems face the challenge of the need to identify the CTCs. Most of the current methods, such as the CellSearch™ system and flow cytometry, are based on fluorescence. They rely on high resolution optical characterization via fluorescent staining, which requires labor-intensive sample manipulation and the detailed qualification of each individual cell. Commercial CellSearch™ systems even require a trained professional to interpret and classify the images obtained to arrive at a number of CTCs. Cost and complexity are major difficulties in the use of these tests for close and frequent follow-ups of patients. On the other hand, microelectronic sensors provide rapid and parallel data acquisition for biological endpoints such as cell attachment and antibody binding (Chen et al., 2008). Apart from their demonstrated capability for system miniaturization and integration, electronic signals such as electrical impedance can be easily recorded and processed to simple outputs for clinical decisions.

The identification of CTCs usually relies on the presence of the epithelial cell adhesion molecule (EpCAM) on the cell membrane (Nagrath et al., 2007; Wang et al., 2009). EpCAM is a pan-epithelial differentiation antigen expressed on the basolateral surface of various human tumor tissues such as stomach, colon, pancreas, gall bladder, bile duct, mammary gland, breast, and lung carcinoma (Chaudry et al., 2007). Fehm et al. (2002) showed that the vast majority of cells expressing epithelial markers in blood from breast, kidney, prostate, and colon cancer patients were aneusomic and

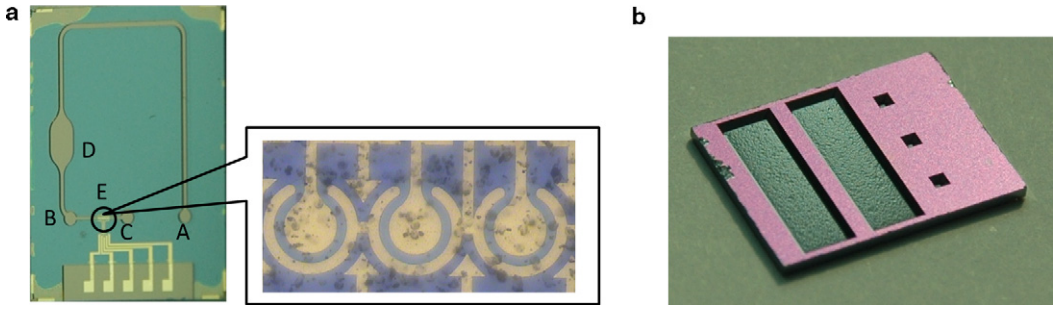

Fig. 2. Design of the microchip: (a) The front side of the detection chip includes microchannels and electrodes: (A) sample inlet, (B) waste outlet during magnetic trapping, (C) waste outlet during cell releasing and washing, (D) magnetic trapping chamber, (E) MEA. Right, a detail of 3 electrodes of the MEA with cancer cells specifically attached to the EpCAM antibody on the top of the electrodes for detection. (b) The backside of the chip shows the etched depression that fits the small magnet used for trapping CTCs.

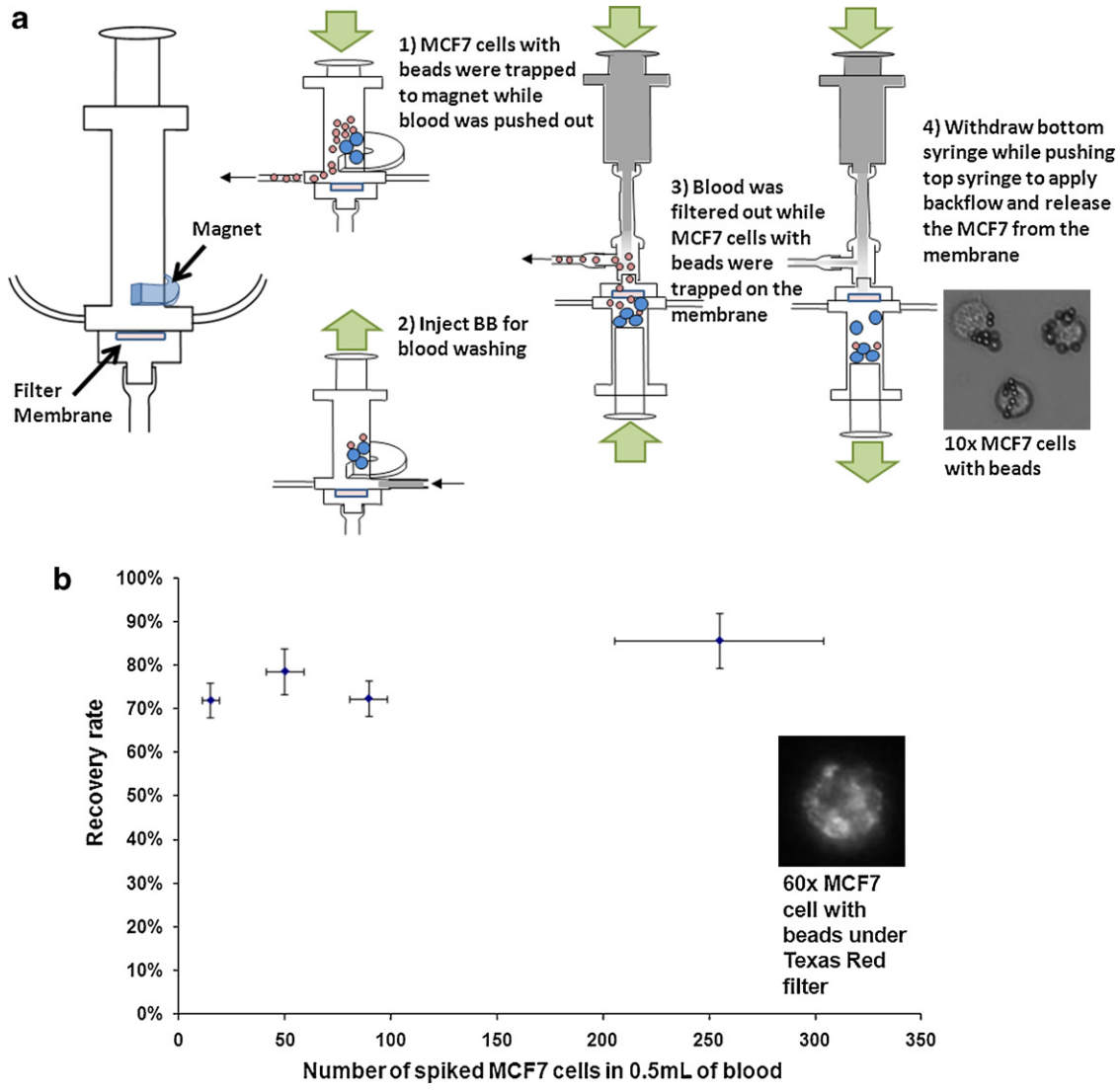

Fig. 3. (a) Schematic design of the filtering syringe and filtration protocol. (b) Recovery rates for different MCF7 cells input numbers. The horizontal error bars are the standard deviation of the number of cells counted in 5 different samples for each experiment, prior to loading it in the chip, while the vertical error bar is the standard deviation for 5 independent experiments.

derived from the primary tumor. Although more detailed analyses of EpCAM roles in CTCs, as well as the potential of other molecules to enhance their 'signature', are needed to increase the precision of diagnostic tools, EpCAM is one of the main clinically relevant indicators for CTC detection.

In this paper, we demonstrate for the first time the electronic (fluorescence-free) detection of CTCs in a convenient semi-integrated system (Fig. 1). The system consists of two modules: cell enrichment and cell identification. CTCs were first enriched by a combination of immunomagnetic isolation (via anti-EpCAM-coated beads) and size filtration in a syringe set-up, amenable to the processing of large blood volumes. The enriched sample was then transferred to the cell identification module where the cells were further concentrated via magnetic sorting in microfluidic channels and captured by antibodies on a microelectrode array (MEA) (Fig. 2). The MEA allowed the trapping of cells on top of the electrodes with negative DEP, their subsequent selection by antibody interactions (EpCAM), and finally detection via impedance spectroscopy. Single electrodes of the MEA achieved a high sensitivity down to 10 cells. This system showed a wider detection range up to hundreds of cells in milliliter-sized blood samples, enabling the follow-up of the changes of the number of CTCs in patients, which is highly demanded for therapy monitoring applications.

2. Materials and methods

2.1. Materials

2.1.1. Chemicals

Toluene, triethylamine, 11-mercaptoundecanoic acid 95% (11-MUA, cat# 450561), 3-mercaptopropionic acid 99% (3-MPA, cat# M580), N-hydroxysuccinimide 97% (NHS, cat# 56480), 1-ethyl-3-(3-dimethylaminopropyl) carbodiimide hydrochloride (EDAC, cat# E6383), and bovine serum albumin (BSA, cat# A3294) were obtained from Sigma–Aldrich. Phosphate buffer solution (PBS, pH = 7.4, calcium chloride and magnesium chloride ions non-present) and the wheat germ agglutinin (WGA) Texas Red®-X conjugate were from Invitrogen. 2-[methoxy(polyethyleneoxy) propyl]trimethoxysilane (Mw = 460–590, silane-PEG) was purchased from Gelest (Morrisville, PA). The fluorescent mounting medium (cat# s3023) was obtained from Dako (USA). Epithelial

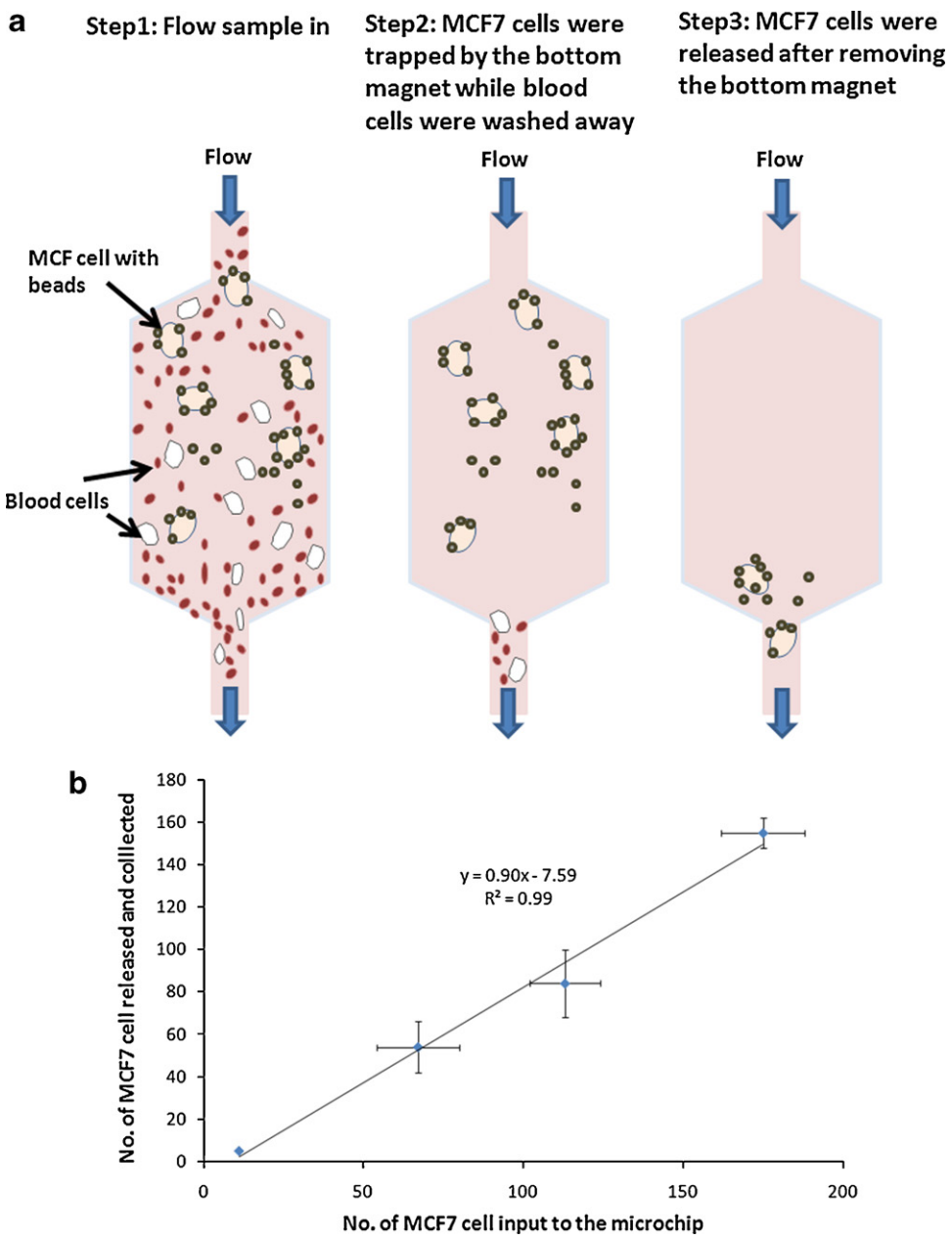

Fig. 4. (a) Schematic protocol for cell enrichment on chip. The cells were first driven into the microchip through a tubing by a syringe pump. Then MCF7 cells were trapped by magnetic force in the trapping chamber while the blood cells were washed away to the waste outlet. Finally, the bottom magnet was removed and the trapped cells were released to the detection area. (b) The graph shows the number of cells released from the magnetic trapping chamber with a flow rate of 25 μL/min versus the number of cells input in the microchip. The horizontal error bars are the standard deviation of the number of cells counted in 3 different samples for each experiment, while the vertical error bars are the standard deviation for 3 independent experiments.

VU-1D9 antibody (EpCAM) (cat# 01420) was from StemCell Technologies Inc. (Vancouver, Canada).

2.1.2. Blocking buffer (BB)

200 mL of BB solution was prepared by adding 10 g Bovine Serum Albumin and 0.5 g HEPES into 150 mL PBS as well as 2 mL Fetal Bovine Serum (FBS) and 0.8 mL EDTA while stirring. Then PBS was added up to make the total volume reach 200 mL. The solution was then adjusted to pH 7.4 and stored at 4 °C.

2.1.3. Cells

MCF7 cells, from a human breast cancer tumor, were purchased from the American Type Culture Collection (ATCC) (cat # HTB-22) and received as frozen vials. They were cultured in Minimum Essential Media (MEM) (Gibco, cat # 11095-080) completed with 10% FBS (Gibco, cat # 10270106), 1 mM sodium pyruvate (Gibco, cat# 11360-070), and 0.1 mM MEM non-essential amino acids (Gibco, cat #11140-050).

2.2. Methods

2.2.1. MCF7 cell enrichment by immunomagnetic isolation and size filtration

The custom-made syringe was filled with 500 μL of human blood diluted with 2 mL of BB containing 2 μL of magnetic beads (4×10^5/μL, 3.28 μm in diameter, Spherotech, Inc., USA) coated with anti-EpCAM (following the manufacturer's protocol) and 10 μL of BB with the desired number of MCF7 cells. The solution was

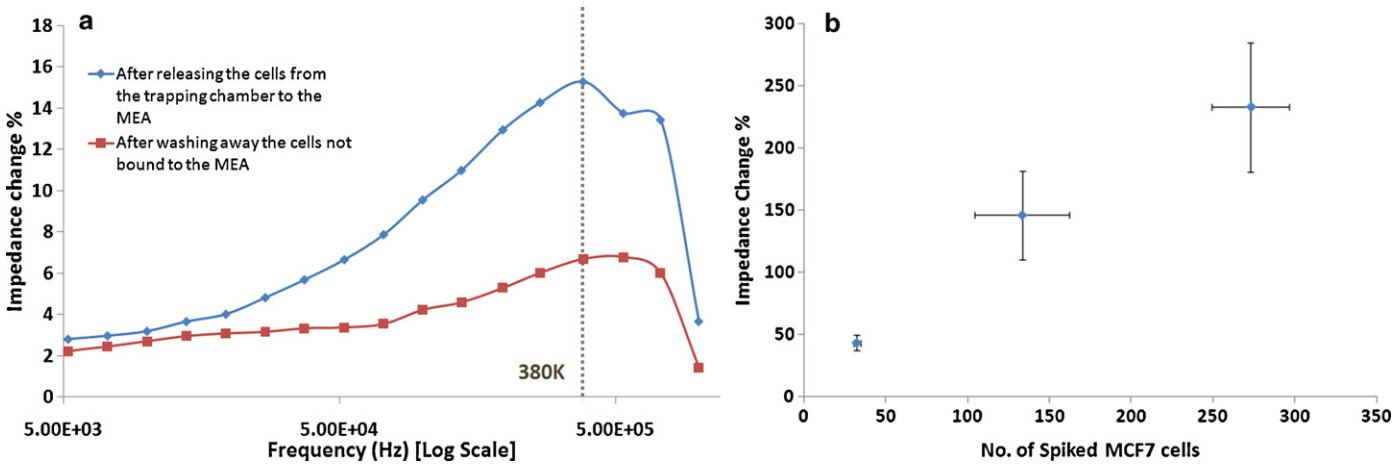

Fig. 5. Integration results: different numbers of MCF7 cells were spiked into the blood samples. The sample was processed through the enrichment and detection in the system. (a) Relative impedance change spectra of a single electrode with respect to frequency for 34 MCF7 cells spiked, after the cells were flowed on the MEA and after the unattached cells were washed away. (b) Impedance change (43 ± 6, 146 ± 36, and $233\% \pm 52$) of all electrodes in the MEA with respect to different numbers of spiked MCF7 cell (30 ± 2, 124 ± 29, 273 ± 23). The horizontal error bars are the standard deviation of the number of cells counted in 3 different samples for each experiment, while the vertical error bar is the standard deviation for 3 independent experiments. The results show that three levels of spiked CTC number could be distinguished by the electronic signal output impedance change ($P < 0.05$ one-way ANOVA).

incubated for 2 h. After incubation, a half ring magnet was affixed to the filter to trap MCF7 cells with magnetic beads while blood was pushed out through a side tube opposite the magnet (Fig. 3(a)). The blocking buffer was then injected through another side-tube to further dilute the blood sample. This process was repeated three times. The following size filtration was performed by using a Whatman Cyclopore track etched membrane (5 μm pore size and 13 mm in diameter). The recovery rate was calculated as the ratio of cells input in the system over the number of cells remaining on the membranes. MCF7 cells were stained with WGA (Alexa 594 – wheat germ agglutinin, Invitrogen, cat# W11262) prior to the experiment and counted under the upright fluorescent microscope Olympus.

2.2.2. Sample transfer after immunomagnetic and size filtration

A tubing (internal diameter 1.5 mm), attached to a 1 mL syringe (BD Precision, USA), was first filled with PBS and used to draw in the filtered sample containing CTCs and another 15 μL of PBS. The tubing was inserted into the inlet on top of the PDMS with the syringe secured to a syringe pump (Fig. 1). For the first 6 s, a flow rate of 150 μL/min was applied to drive most of cells into the microchip followed by a flow rate of 10 μL/min for flowing cells to the trapping chamber.

2.2.3. Magnetic trapping

The microchip together with the PDMS was mounted onto a custom-made fixture with an acrylic piece to secure the set-up and prevent leakage. A bar magnet was placed into the etched depression (slider) on the back side of the microchip (Fig. 2). After immunomagnetic isolation and size filtering, the filtered samples were driven into the microchip through a tubing (1.5 mm in diameter) by a syringe pump. To further separate CTCs from blood cells, the magnetic force trapped MCF7 cells labeled with magnetic beads while blood cells passed by and flew to the waste outlet. Finally, the bottom magnet was removed and the trapped cells were released to the MEA for detection.

2.2.4. DEP application and cell trapping on the electrodes

The released cells in the detection chamber were subjected to negative DEP (0.6 V, 1 MHz) to concentrate them to the centre of the gold electrodes (Fig. 2). All working electrodes were shorted together to function as a single DEP electrode. MCF7 cells were then incubated onto the surface to bind to anti-EpCAM antibodies. Unattached cells (from blood) and beads were washed away by PBS (flow rate 25 μL/min), leaving MCF7 cells on the gold electrodes.

2.2.5. Impedance measurement

The impedance detection set-up consisted of a test jig, connection wires, and an impedance measurement system (IvumStat Impedance Analyzer, Ivum Technologies, Netherlands) controlled by a computer. The impedance was measured from individual electrodes with respect to the shorted horse-shoe shaped counter/reference electrodes using a conventional 2-electrodes scheme, at amplitude of 0.05 V. The frequencies ranged from 100 Hz to 10^6 Hz with 29 data points (7 points per decade).

3. Results and discussions

3.1. Cell enrichment in the filter syringe by immunomagnetic isolation and size filtration)

The first function that the full system performed was the enrichment of cancer cells, represented here by MCF7 cells, which was achieved through a combination of immunomagnetic isolation and size filtration. The immunomagnetic isolation provides a simple and sensitive way to isolate cells expressing specific antibodies (Allard et al., 2004). Magnetic beads coated with anti-EpCAM antibodies were used to bind and isolate MCF7 cells, which highly expressed the EpCAM antigen. Size filtration was applied as a second step to get rid of smaller blood cells and beads. The specific protocol employed is detailed in Fig. 3(a).

Due to the complex nature of blood, the protocols to achieve suitable magnetic selection for the detection of rare circulating cells had to be optimized thoroughly. For example, Kagan et al. (2002) used nanometer-sized particles (or 'ferrofluid') to fish out the EpCAM positive cells, increasing the number of beads in the sample which resulted in increased labeling. Talasaza et al. (2008) utilized another approach to increase the magnetic force by introducing the magnet directly in the solution. In this work, our combined system provides various advantages. On the one hand, the use of magnetic concentration decreases the complexity of the sample, which is then easier to filter through the membrane pores. While the size filter developed by Vona et al. (2000) needs to dilute the sample excessively (10× dilution), this first immunomagnetic treatment allowed us to process the sample with only 4× dilution on input.

Therefore, the total processing volume was decreased 2.5× when compared with Vona et al. (2000). On the other hand, the use of a pore-size filter after immunomagnetic isolation not only eliminates blood cells, but also unbound beads, leaving a cell suspension easier to handle in a microfluidic system. Conversely, the cell-bead complexes are larger in size than simple cells and increase the selectivity of the filter. The integration of both functions together in this cell enrichment module is an example of the fact that integrated devices can often achieve more than the sum of each individual method.

To balance the interplay between the two functions, an optimization of the critical parameters was carried out. Commercial polycarbonate filters with different pore sizes (5, 8, and 10 μm in diameter) were tested as well as different magnetic bead sizes (1, 3.28, and 6 μm in diameter). Results (in supplementary data C and D) were in favor of a filter with 5 μm pore size (Whatman, USA) and beads with 3.28 μm (Spherotech, Inc., USA) in diameter, which had the best recovery rate for size filtration as well as the best on-chip trapping efficiency. These results contrast slightly with the design presented by Vona et al. (2000), who used 8 μm. In the present work, the use of a smaller pore size increased the sensitivity, while the combination with immunomagnetic isolation increased the selectivity. Using these parameters, blood samples (0.5 mL) were processed and the recovery rate was calculated for different numbers of spiked cancer cells (Fig. 3(b)). Overall efficiencies reached 70–90%. Even when spiking only 10 MCF7 cells into 0.5 mL of blood, more than 70% of MCF7 cells were recovered. This compares favorably with the reports of a microchip with microposts to capture CTCs from whole blood (Nagrath et al., 2007), in which a recovery efficiency >60% was achieved with 50–50,000 cells spiked per milliliter of blood. The conventional benchtop method by Kagan et al. (2002) was reported to achieve 77.1% when using control cells.

3.2. Cell enrichment on the microchip

To facilitate cell detection by impedance measurement, the filtered sample was introduced into a microchip for further enrichment (Figs. 1 and 2). In a similar fashion as the combination of immunomagnetic isolation and size filtration, two functions in one module, we present a synergy of trapping, concentration, and detection on a single microchip, which demanded specific design rules and process parameters. Fig. 2(a) shows the fabricated microchip with the microfluidic channel leading to a trapping chamber before the MEA for detection. The backside etched depression in the chip (Fig. 2(b)) allowed positioning the magnet right under the trapping chamber and close to the cells, thus increasing the trapping force and enabling convenient processing of flow rates. In the trapping chamber, the bottom magnet trapped the cancer cells bound with magnetic beads, while most blood cells remaining from the filtration module were washed away to the waste outlet (Fig. 4(a)).

The cell trapping efficiency was calculated as the number of cells trapped over the total number of cell input. Results show that an average of 90% of MCF7 cells were trapped (Fig. 4(b)). Horizontal error bars in Fig. 4(b) are the standard deviation of the number of cells input inside the sample. They arose from the difficulty of getting exact numbers of cells from cell suspensions by dilution for such low numbers. It can be noted that the fitted linear regression crosses the *x*-axis at a positive value (approximately 8 cells), representing an estimation of the number of cells lost during the process. It represents a theoretical limitation of the system that would not be able to detect less than the number of cells lost during the enrichment process, independently of the errors imparted during the detection. This number corresponds to the threshold of detection for diagnosis of metastatic breast cancer (Allard et al., 2004) for a sample of 12 ml of blood and is much smaller than the number reported by Pachmann et al. (2005a,b) for therapy monitoring (50/ml), meaning that this system is well-suited for these applications. After removing the blood cells, the bottom magnet was removed and cells with magnetic beads were released and flew down from the trapping chamber to the MEA for detection (Fig. 4(a)). The volume of the detection chamber (5 μL) was designed to accommodate all the liquid coming for the release of the cells so that no cancer cells were lost in the channels.

3.3. Detection of MCF7 cells on the MEA by impedance

Detecting a small number of cells, such as CTCs, via impedance measurements on the MEA requires a high sensitivity. This can be achieved by using microelectrodes with a diameter below 100 μm (Chen et al., 2008; Ng et al., 2010). However, this translated into tight constraints in terms of specificity, since other cells attached on the electrodes would give rise to a non-negligible impedance signal and limit space for CTC adhesion. Here we selected and concentrated CTCs specifically on the MEA through coupled magnetic trapping (as described in Section 3.2) and immunochemical capture.

Impedance measurement was performed before and after MCF7 cells were captured onto the MEA. Fig. 5(a) shows the analysis of the impedance change (modulus part) of a single electrode at different time points, t, in the experiment, compared to the baseline in buffer, $\Delta Z(t)_{\%} = (Z(t) - Z_{\text{baseline}})/Z_{\text{baseline}} \times 100$), in a similar fashion as in our previous work (Ng et al., 2010). Although other descriptors of the impedance (the phase, the module, the imaginary part for example) also show specific changes with regards to the presence of the cells, the modulus part was the most sensitive in our studies and will be used to report the signal. As expected, the impedance, when cells were released from the magnetic trapping chamber and directed to the MEA surface by negative DEP, was higher than when only buffer was present (PBS) (Wegener et al., 2000). After washing with buffer, the signal decreased as EpCAM negative cells did not bind to the surface and were removed, leaving only the specific cancer cells on the MEA.

Different cell types have different frequencies at which the contribution of the cells attached on the electrodes to the impedance of the system is maximum (Rümenapp et al., 2009). In Fig. 5(a), the maximum percentage change in impedance was observed to occur at a frequency around $\log_{10}5.73$ (533 kHz) for MCF7 cells. Hence, we used this frequency to monitor the detection of the cancer cells on the MEA. Although other descriptors of the impedance (the phase, the real part, the imaginary part for example) also show specific changes with regards to the presence of the cells, the modulus was the most sensitive in our studies and will be used to report the signal.

To demonstrate the capability of our CTC detection system and to realize a complete analysis of blood samples, different numbers of MCF7 cells were spiked into 0.5 mL blood samples. The samples were processed through the full system (both cell enrichment module and cell identification module) and the impedance change was recorded for each individual electrode of the MEA and added up. Fig. 5b shows that three levels of spiked CTC number (30 ± 2, 124 ± 29, 273 ± 23) were distinguished by impedance change ($P < 0.05$, one-way ANOVA). Although the detection was performed on an antibody coated surface to minimize the influence of other species contained of the samples on the impedance measurements (Ng et al., 2010), nonspecific fouling has always been a concern for such biosensors. Here, we used a semi-integrated sample purification process, namely filtration (size separation), immunomagnetic trapping of CTC, and washing, to reduce the interference of blood components and enable the specific detection of the cancer cells. Extensive washes were performed after the cancer cells were trapped and attached to the surface of

the chip. These rinses would clean the blood constituents non-specifically adsorbed on the surface, The results further show that the impedance signal increased with increased CTC numbers, while other blood constituents (cells and molecules) were kept constant (same blood sample), an expected trend for specific cancer cell detection. These results confirm the capability of this system to be used for therapy monitoring, where small numbers of CTCs have to be detected from large blood samples, to inform doctors on the increase or decrease of this biomarker. While other techniques are mostly based on CTC thresholds for diagnostic applications (Cristofanilli et al., 2004), our integrated system enables highly sensitive detection as well as the electronic differentiation of different cell numbers.

4. Conclusion

In this paper, we have reported the development of a two-module system based on the electronic detection of rare circulating tumor cells from large blood samples through a combination of immunomagnetic isolation and size filtration in a convenient syringe-based device, coupled to a microchip specifically detecting cancer cells by impedance measurement. The integration of different techniques into a single system led to synergistic effects, resulting in the detection of few cells in a large blood sample, with the added ability to differentiate between levels of cell numbers. The unique association of these capabilities facilitated a reconciliation between the macro-world of large blood samples and the micro-world of high sensitive label-free detection in lab-on-chips, showing a high potential of being readily used for therapy monitoring applications in the hospital.

Appendix A. Supplementary data

Supplementary data associated with this article can be found, in the online version, at doi:10.1016/j.bios.2010.10.048.

References

Allard, W.J., Matera, J., Miller, M.C., Repollet, M., Connelly, M.C., Rao, C., Tibbe, A.G.J., Uhr, J.W., Terstappen, L.W.M.M., 2004. Clinical Cancer Research 10, 6897–6904.
Baker, M.K., Mikhitarian, K., Osta, W., Callahan, K., Hoda, R., Brescia, F., Kneuper-Hall, R., Mitas, M., Cole, D.J., Gillanders, W.E., 2003. Clinical Cancer Research 9 (13), 4865–4871.
Benez, A., Geiselhart, A., Handgretinger, R., Schiebel, U., Fierlbeck, G., 1999. Journal of Clinical Laboratory Analysis 13, 229–233.
Chaudry, M.A., Sales, K., Ruf, P., Lindhofer, P., Winslet, M.C., 2007. British Journal of Cancer 96, 1013–1019.
Chen, Y., Zhang, J., Wang, Y., Zhang, L., Julien, R., Tang, K., Balasubramanian, N., 2008. Biosensors and Bioelectronics 23 (9), 1390–1396.
Cristofanilli, M., Budd, G.T., Ellis, M.J., Stopeck, A., Matera, J., Miller, M.C., Reuben, J.M., Doyle, G.V., Allard, W.J., Terstappen, L.W.M.M., Hayes, D.F., 2004. The New England Journal of Medicine 351 (8), 781–791.
Fan, T., Zhao, Q., Chen, J.J., Chen, W.T., Pearl, M.L., 2009. Gynecologic Oncology 112, 185–191.
Fehm, T., Sagalowsky, A., Clifford, E., Beitsch, P., Saboorian, H., Euhus, D., Meng, S., Morrison, L., Tucker, T., Lane, N., Ghadimi, B.M., Heselmeyer-Haddad, K., Ried, T., Rao, C., Uhr, J., 2002. Clinical Cancer Research 8, 2073–2084.
Gascoyne, P.R.C., Noshari, J., Anderson, T.J., Becker, F.F., 2009. Electrophoresis 30, 1388–1398.
Hayes, D.F., Cristofanilli, M., Budd, G.T., Ellis, M.J., Stopeck, A., Miller, M.C., Matera, J., Allard, W.J., Doyle, G.V., Terstappen, L.W., 2006. Clinical Cancer Research 12 (14), 4218–4224.
Hüsemann, Y., Geigl, J.B., Schubert, F., Musiani, P., Meyer, M., Burghart, E., Forni, G., Eils, R., Fehm, T., Riethmüller, G., Klein, C.A., 2008. Cancer Cell 13 (1), 58–68.
Kagan, M., Howard, D., Bendele, T., Mayes, J., Silvia, J., Repollet, M., Doyle, J., Allard, J., Tu, N., Bui, T., Russell, T., Rao, C., Hermann, M., Rutner, H., Terstappen, L.W.M.M., 2002. Journal of Clinical Ligand Assay 25, 104–110.
Nagrath, S., Sequist, l.V., Maheswaran, S., Bell, D.W., Irimia, D., Ulkus, L., Smith, M.R., Kwak, E.L., Digumarthy, S., Muzikansky, A., Ryan, P., Balis, U.J., Tompkins, R.G., Haber, D.A., Toner, M., 2007. Nature 450, 1235–1239.
Ng, S.Y., Reboud, J., Wang, K.Y.P., Tang, K.C., Zhang, L., Wong, P., Moe, K.T., Shim, W., Chen, Y., 2010. Biosensors and Bioelectronics 25 (5), 1095–1101.
Pachmann, K., Camara, O., Kavallaris, A., Schneider, U., Schünemann, S., Höffken, K., 2005a. Breast Cancer Research 7, R975–R979.
Pachmann, K., Clement, J.H., Schneider, C.P., Willen, B., Camara, O., Pachmann, U., Höffken, K., 2005b. Clinical Chemistry and Laboratory Medicine 43 (6), 617–627.
Rümenapp, C., Remm, M., Wolf, B., Gleich, B., 2009. Biosensors and Bioelectronics 24, 2915–2919.
Talasaza, A.H., Powellc, A.A., Huber, D.E., Berbeeb, J.G., Rohd, K., Yu, W., Xiao, W., Davis, M.M., Peasea, R.F., Mindrinos, M.N., Jeffrey, S.S., Davis, R.W., 2008. Proceedings of the National Academic Sciences of the United States of America 196 (10), 3970–3975.
Vona, G., Sabile, A., Louha, A., Sitruk, V., Romana, S., Schutze, K., Caproni,.F., Franco, D., Pazzagli, M., Vekemans, M., Lacour, B., Brechot, C., Paterlini-Brechot, P., 2000. American Journal of Pathology 156, 57–63.
Wang, S., Wang, H., Jiao, J., Chen, K.J., Owens, G.E., Kamei, K.I., Sun, J., Sherman, D.J., Behrenbruch, C.P., Wu, H., Tseng, H.R., 2009. Angewandte Chemie-International Edition 48, 8970–8973.
Wegener, J., Keese, C.R., Giaever, I., 2000. Experimental Cell Research 259 (1), 158–166.
Zheng, S., Lin, H., Liu, J.Q., Balic, M., Datar, R., Cote, R.J., Tai, Y.C., 2007. Journal of Chromatography A 1162, 154–161.